AIAA JOURNAL
Vol. 40, No. 5, May 2002

Free In-Plane Vibration of Rectangular Plates

Gang Wang* and Norman M. Wereley†
University of Maryland, College Park, Maryland 20742

Based on the Kantorovich–Krylov variational method (Kantorovich, L. V., and Krylov, V. I., *Approximate Methods of Higher Analysis*, Noordhoff International, Groningen, The Netherlands, 1964, pp. 241–357), we analytically solve for modal frequency and displacement mode shapes of in-plane vibration of rectangular plates with free and clamped boundary conditions. Free and clamped boundary conditions do not allow closed-form solutions from partial differential equations. We develop analytical expressions of plate mode shapes consisting of a linear combination of progressive waves with unknown wave amplitudes. We then use these to calculate the modal frequencies and the wave amplitudes with analytical mode shape expressions. An iteration scheme is presented to calculate efficiently the natural frequency and corresponding mode shape functions based on the Kantorovich–Krylov method. Three configurations are considered: a plate with four edges clamped, a plate with three edges clamped and one edge free, and a plate with two parallel edges clamped and the other two edges free. The first six natural frequencies predicted by our approach are validated using NASTRAN and other analyses from the literature. Improvements in accuracy of the first six predicted natural frequencies were achieved using the Kantorovich–Krylov method when compared against other results in the literature.

Nomenclature

a	=	length of plate in x direction
b	=	length of plate in y direction
E	=	Young's modulus of plate material
h	=	plate thickness
$k_{1,2}$	=	two wave numbers in the solution of mode shape functions
m, n	=	number of half-wavelengths for mode shapes
N_ζ	=	nondimensional normal stress in x direction
$N_{\zeta,\eta}$	=	nondimensional shear stress
N_η	=	nondimensional normal stress in y direction
u	=	displacement in x direction
v	=	displacement in y direction
X_u	=	separable component of a mode shape function for u in x direction
X_v	=	separable component of a mode shape function for v in x direction
Y_u	=	separable component of a mode shape function for u in y direction
Y_v	=	separable component of a mode shape function for v in y direction
α	=	ratio of length in x and y direction
ζ	=	nondimensional length in x direction
η	=	nondimensional length in x direction
ν	=	Poisson's ratio of plate
ρ	=	density of plate
Ω	=	nondimensional frequency
Ω_x	=	nondimensional frequency solution in x direction
Ω_y	=	nondimensional frequency solution in y direction
ω	=	excitation frequency

Received 17 March 2001; presented as Paper 2001-1476 at the AIAA Structures, Structural Dynamics, and Materials Conference, Seattle, WA, 16–20 April 2001; revision received 10 July 2001; accepted for publication 10 December 2001.

*Research Associate, Smart Structures Laboratory, Alfred Gessow Rotorcraft Center, Department of Aerospace Engineering; gwang@glue.umd.edu. Member AIAA.

†Associate Professor of Aerospace Engineering, Smart Structures Laboratory, Alfred Gessow Rotorcraft Center, Department of Aerospace Engineering; wereley@eng.umd.edu. Associate Fellow AIAA.

Introduction

FREE in-plane vibration of a rectangular plate is investigated. The transverse bending vibration of plates has received much attention in the literature.[1,2] Results are available for transverse bending frequencies and mode shapes for a wide range of plate shapes and boundary conditions. Usually, for the rectangular plate case, plate bending mode shapes are the expansion of beam bending modes in both the x and y directions with weighted coefficients calculated using the Rayleigh–Ritz method. The closed-form plate bending mode shapes are available only for the Levy type of rectangular plates, that is, at least two parallel edges with simply supported boundary conditions (see Ref. 3). However, in addition to transverse bending or out-of-plane vibration, a plate can also undergo in-plane vibration, namely, plane longitudinal and shear motions. Improving the understanding of modal characteristics of in-plane plate vibrations is a key goal of this paper. In-plane plate mode shapes are very important for the analysis of complicated plate structures, such as a folded plate in space structures[4] and sandwich plates.[5] For our particular interests, we need to calculate the bending frequencies and response of three-layered sandwich plate structures, where a viscoelastic core is sandwiched between two face plates for damping augmentation. The energy is dissipated by shear deformations in the viscoelastic damping core, which causes a coupling of in-plane and bending motions for each face plate. The analysis of this type of plate structure involves both in-plane and bending mode shapes when using assumed modes methods. As discussed in Ref. 5, the in-plane modes are critical when evaluating the bending frequencies of sandwich plates. Therefore, free in-plane plate vibration becomes the topic of this paper. Our goal is to calculate the in-plane plate mode shapes directly, instead of using rod mode shapes in both the x and y directions. We have shown that these updated in-plane plate mode shapes improve the accuracy of frequency predictions and lower the computational cost due to the large number of rod modes involved in our sandwich plate analysis.[6]

Few studies have focused on the study of in-plane vibration of rectangular plates. Closed-form solutions exist only for simply supported boundary condition cases as shown in Ref. 7. However, clamped and free boundary conditions are typically encountered in applications. Recently, Farag and Pan[8] presented forced responses of in-plane vibration of a rectangular plate under in-plane point excitation with four-edge clamped boundary conditions. The modal frequencies were calculated by using the first 10 assumed rod mode shapes in both the x and y directions. This involves an eigenvalue problem with a matrix of order 200. The analysis was validated using NASTRAN with 480 four-node plane elements. In a subsequent study, Farag and Pan[9] discussed modal characteristics of a rectangular plate with two parallel edges clamped, whereas the other two

edges are either both clamped (CCCC), both free (CFCF), or one clamped and one free (CCCF). For these rectangular plate configurations, two parallel edges are always clamped. Then sine functions can be assumed to be the one separable part in the solution of the mode shape function. Substituting this solution into the governing equations of motion, the two-dimensional problem can be reduced to one-dimensional problem in terms of another part of separable solution. An iteration scheme was developed to calculate modal frequencies. They presented the natural frequencies for the three boundary condition cases mentioned and each validated by using NASTRAN solutions. The maximum error in the in-plane vibration modal frequency was 4.6% for CCCC case, 8.4% for CCCF case, and 12% for CFCF case, in which the first eight modes were considered. The coefficients of mode shapes were determined numerically by an iteration scheme, but these coefficient results were not presented.

In our analysis, we also examine modal characteristics of a rectangular plate undergoing in-plane vibration. We will calculate the natural frequencies and the mode shapes for displacement u and v based on the Kantorovich–Krylov method.[10] We will directly solve for modal frequencies and corresponding mode shapes instead of using rod mode shapes to approximate both the x and y directions. Separable solutions were assumed to solve analytically for all displacements. This method has been successfully applied to plate bending vibration analysis.[11] The equilibrium position of a mechanical system is the position corresponding to the minimum potential energy. Thus, the problem of solving the boundary value problem for the partial differential equations (PDEs) is equivalent to the problem of finding the function minimizing the integral of total potential energy. This equivalence enables us to solve the PDEs by minimizing the total energy. The most familiar method is the Rayleigh–Ritz method. However, this method provides only approximate solutions of PDEs because the assumed mode shapes are only admissible functions. The Galerkin method can provide good approximations for PDEs, if we can find a function such that it satisfies both the geometric and force boundaries. Fortunately, the Kantorovich–Krylov variational method provides a method of determining higher-order solutions for PDEs. This method can reduce PDEs to ordinary differential equations (ODEs), so that we can solve these ODEs to determine the mode shape functions analytically. An iteration scheme is developed to calculate the modal frequencies and coefficients of the corresponding mode shape functions.

Our approach for in-plane vibration analysis will be validated using NASTRAN results and the results in Ref. 9. We will consider three configurations of rectangular plates: CCCC, CCCF, and CFCF cases. The first six modal frequencies of in-plane vibration will be calculated and compared to available results. The mode shapes will be plotted in vector form to show the natural modes of in-plane vibration of rectangular plates.

Analysis

In this section, we present the expressions describing potential energy of in-plane rectangular plate vibrations under the harmonic excitation. The variation of the total energy is shown, which corresponds to the governing equations and associated boundary conditions for in-plane plate vibrations. Separable solutions are assumed for in-plane displacements u and v. Based on the Kantorovich–Krylov[10] iterative method, mode shapes and modal frequencies can be iteratively calculated until convergence is achieved.

System Energy and Equations

The rectangular plate is illustrated in Fig. 1. The potential energy for in-plane vibration is

$$U = \frac{1}{2}\int_0^a \int_0^b \left\{ \frac{Eh}{1-\nu^2}\left[\left(\frac{\partial u}{\partial x}\right)^2 + \left(\frac{\partial v}{\partial y}\right)^2 + 2\nu \frac{\partial u}{\partial x}\frac{\partial v}{\partial y} + \frac{1}{2}(1-\nu)\left(\frac{\partial u}{\partial y} + \frac{\partial v}{\partial x}\right)^2 \right] - \rho h \omega^2 (u^2 + v^2) \right\} \mathrm{d}x\, \mathrm{d}y \qquad (1)$$

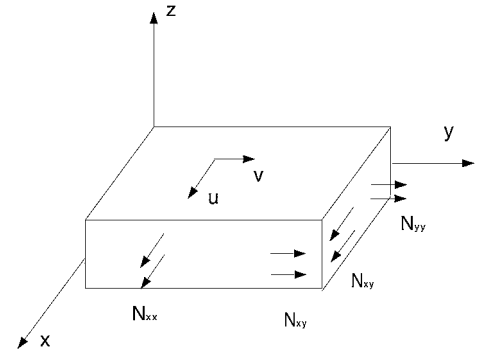

Fig. 1 Schematic of rectangular plate under in-plane vibration.

We took the variation of the preceding total energy and performed integration by parts, assuming that the variation of the total energy is equal to zero. This yields the governing equations and associated boundary conditions for in-plane plate vibration. Here, nondimensional results are shown:

$$-\delta U = 0 = \int_0^1 \int_0^1 \left[\frac{\partial^2 u}{\partial \zeta^2} + \frac{1}{2}\alpha^2(1-\nu)\frac{\partial^2 u}{\partial \eta^2} + \frac{1}{2}\alpha(1+\nu)\frac{\partial v^2}{\partial \zeta\, \partial \eta} + \Omega^2 u \right] \delta u \, \mathrm{d}\zeta \, \mathrm{d}\eta + \int_0^1 \int_0^1 \left[\frac{1}{2}(1-\nu)\frac{\partial^2 v}{\partial \zeta^2} + \alpha^2 \frac{\partial^2 v}{\partial \eta^2} + \frac{1}{2}\alpha(1+\nu)\frac{\partial u^2}{\partial \zeta\, \partial \eta} + \Omega^2 v \right] \delta v \, \mathrm{d}\zeta \, \mathrm{d}\eta - \int_0^1 (N_\zeta \delta u)|_{\zeta=0}^1 \, \mathrm{d}\eta - \int_0^1 (N_{\zeta\eta}\delta v)|_{\zeta=0}^1 \, \mathrm{d}\eta - \int_0^1 (N_\eta \delta v)|_{\eta=0}^1 \, \mathrm{d}\zeta - \int_0^1 \alpha (N_{\zeta\eta}\delta u)|_{\eta=0}^1 \, \mathrm{d}\zeta \qquad (2)$$

where the nondimensional parameters are

$$\zeta = x/a, \qquad \eta = y/b, \qquad \alpha = a/b$$

$$\Omega^2 = \rho \omega^2 a^2 (1-\nu^2)/E$$

and the nondimensional normal forces are

$$N_\zeta = \frac{\partial u}{\partial \zeta} + \alpha\nu\frac{\partial v}{\partial \eta}, \qquad N_\eta = \alpha^2 \frac{\partial v}{\partial \eta} + \alpha\nu\frac{\partial u}{\partial \zeta}$$

$$N_{\zeta\eta} = \frac{1}{2}(1-\nu)\left(\alpha\frac{\partial u}{\partial \eta} + \frac{\partial v}{\partial \zeta}\right)$$

Note that Eq. (2) is the weak or variational form of the PDEs,[12] together with all possible boundary conditions existing along four edges for in-plane plate vibration.

Solution

Determining plate mode shapes u and v satisfying Eq. (2) is equivalent to solving the boundary value problem for in-plane plate vibration. We wish to find functions that exactly satisfy Eq. (2). This gives us the closed-form solutions of in-plane plate vibration. This method is called the Kantorovich–Krylov[10] method. A numerical scheme is used to solve a set of ODEs with associated boundary conditions to achieve a value of zero for the variation of total energy. To do this, we assume a separable solution for displacements u and v for a mode (mode number is neglected in all derivations):

$$u(\zeta, \eta) = X_u(\zeta) Y_u(\eta) \qquad (3)$$

$$v(\zeta, \eta) = X_v(\zeta) Y_v(\eta) \qquad (4)$$

If we assume that the pair Y_u and Y_v are prescribed a priori, we will obtain

$$\delta u = Y_u \delta X_u \qquad (5)$$

$$\delta v = Y_v \delta X_v \qquad (6)$$

Substituting Eq. (3–6) into Eq. (2) and performing integration along η direction yields

$$-\delta U = 0 = \int_0^1 \left(a_1 \frac{d^2 X_u}{d\zeta^2} + a_2 \frac{dX_v}{d\zeta} + a_3 X_u\right)\delta X_u \, d\zeta + \int_0^1 \left(b_1 \frac{d^2 X_v}{d\zeta^2} + b_2 \frac{dX_u}{d\zeta} + b_3 X_v\right)\delta X_v \, d\zeta - \int_0^1 (N_\zeta Y_u \delta X_u)|_{\zeta=0}^1 \, d\eta - \int_0^1 (N_{\zeta\eta} Y_v \delta X_v)|_{\zeta=0}^1 \, d\eta \quad (7)$$

The coefficients a_k and b_k are

$$a_1 = \int_0^1 Y_u^2 \, d\eta$$

$$a_2 = \int_0^1 \frac{1}{2}(1+\nu)\alpha \frac{dY_v}{d\eta} Y_u \, d\eta - \frac{1}{2}(1-\nu)\alpha \, (Y_v Y_u)|_{\eta=0}^1$$

$$a_3 = \int_0^1 \left[\alpha^2 \frac{1}{2}(1-\nu)\frac{d^2 Y_u}{d\eta^2} Y_u + \Omega^2 Y_u^2\right] d\eta - \frac{1}{2}(1-\nu)\alpha^2 \left(\frac{dY_u}{d\eta} Y_u\right)\Big|_{\eta=0}^1$$

$$b_1 = \int_0^1 \frac{1}{2}(1-\nu) Y_v^2 \, d\eta$$

$$b_2 = \int_0^1 \frac{1}{2}(1+\nu)\alpha \frac{dY_u}{d\eta} Y_v \, d\eta - \nu\alpha (Y_u Y_v)|_{\eta=0}^1$$

$$b_3 = \int_0^1 \left(\alpha^2 \frac{d^2 Y_v}{d\eta^2} Y_v + \Omega^2 Y_v^2\right) d\eta - \alpha^2 \left(\frac{dY_v}{d\eta} Y_v\right)\Big|_{\eta=0}^1$$

Equation (7) corresponds to two coupled ODEs and associated boundary conditions in terms of X_u and X_v. The two equations are

$$a_1 \frac{d^2 X_u}{d\zeta^2} + a_2 \frac{dX_v}{d\zeta} + a_3 X_u = 0 \quad (8)$$

$$b_1 \frac{d^2 X_v}{d\zeta^2} + b_2 \frac{dX_u}{d\zeta} + b_3 X_v = 0 \quad (9)$$

The boundary conditions at $\zeta = 0$ and 1 are needed. For a clamped edge

$$X_u = X_v = 0 \quad (10)$$

For a free edge

$$a_1 \frac{dX_u}{d\zeta} + a_{22} X_v = 0 \quad (11)$$

$$b_{11} \frac{dX_v}{d\zeta} + b_{22} X_u = 0 \quad (12)$$

where

$$a_{22} = \int_0^1 \nu\alpha \frac{dY_v}{d\eta} Y_u \, d\eta, \qquad b_{11} = \int_0^1 Y_v^2 \, d\eta$$

$$b_{22} = \int_0^1 \alpha \frac{dY_u}{d\eta} Y_v \, d\eta$$

We now have two ODEs along with associated boundary conditions in terms of X_u and X_v. Before we solve these, we list some observations:

1) From the earlier expressions of coefficients, we note that $a_2 = -b_2$. This is due to the physical symmetric property of coupling terms in the PDEs. Mathematically, this can be illustrated by performing integration by parts for either a_2 and b_2.

2) Two ODEs in Eqs. (8) and (9) are coupled only if nonzero values of a_2 and b_2 exist.

3) The boundary conditions are always coupled in terms of X_u and X_v, except in the case of a clamped edge. Therefore, it is possible to find the uncoupled mode shapes for four clamped edges if the coupling terms in two ODEs are zero, in which a_2 and b_2 are zero. However these mode shape functions are meaningless because they are only admissible functions. However, when a free edge is introduced, uncoupled mode shapes no longer exist because the boundary conditions [Eqs. (11) and (12)] are coupled in terms of X_u and X_v.

Uncoupled and coupled mode shapes were also discussed by Farag and Pan.[9] We will concentrate on solutions of coupled mode shapes. In-plane plate vibration should be coupled for both mode shapes of u and v because of nonzero Poisson ratio effects and shear deformation, which is a function of both displacements u and v. We can rewrite Eq. (8) in terms of either X_u or X_v, as

$$\frac{d^4 X_u}{d\zeta^4} + 2p \frac{d^2 X_u}{d\zeta^2} + q X_u = 0 \quad (13)$$

or

$$\frac{d^4 X_v}{d\zeta^4} + 2p \frac{d^2 X_v}{d\zeta^2} + q X_v = 0 \quad (14)$$

where

$$p = \tfrac{1}{2}[-(a_2 b_2 / a_1 b_1) + b_3/b_1 + a_3/a_1], \qquad q = a_3 b_3 / a_1 b_1$$

The solutions for X_u and X_v can be written as a wave expansion:

$$X_u = c_1 e^{-k_1\zeta} + c_2 e^{k_1\zeta} + c_3 e^{-k_2\zeta} + c_4 e^{k_2\zeta} \quad (15)$$

$$X_v = d_1 e^{-k_1\zeta} + d_2 e^{k_1\zeta} + d_3 e^{-k_2\zeta} + d_4 e^{k_2\zeta} \quad (16)$$

Here, c_1, c_2, c_3, and c_4 are four independent wave coefficients, and d_1, d_2, d_3, and d_4 can be expressed in terms of c_1, c_2, c_3, and c_4 from Eq. (8). Also, k_1 and k_2 are characteristic roots of Eq. (13) and are given by

$$k_1^2 = -p + \sqrt{p^2 - q} \quad (17)$$

$$k_2^2 = -p - \sqrt{p^2 - q} \quad (18)$$

For plate in-plane vibration, There are two kinds of waves traveling across the plate. One is a longitudinal wave along the x and y directions; the other is a shearing wave. This means that we have two different wave numbers as in Eqs. (17) and (18). Because there is no damping introduced in the system, the roots k_1 and k_2 can not be complex numbers. The analytical expressions of mode shapes X_u and X_v are given hereafter based on the possible signs of characteristic roots k_1^2 and k_2^2.

1) If $k_1^2 > 0$ and $k_2^2 > 0$, then

$$X_u = c_1 \sinh(k_1\zeta) + c_2 \cosh(k_1\zeta) + c_3 \sinh(k_2\zeta) + c_4 \cosh(k_2\zeta)$$

$$X_v = d_1 \sinh(k_1\zeta) + d_2 \cosh(k_1\zeta) + d_3 \sinh(k_2\zeta) + d_4 \cosh(k_2\zeta)$$

2) If $k_1^2 > 0$ and $k_2^2 < 0$, then

$$X_u = c_1 \sinh(k_1\zeta) + c_2 \cosh(k_1\zeta) + c_3 \sin(|k_2|\zeta) + c_4 \cos(|k_2|\zeta)$$

$$X_v = d_1 \sinh(k_1\zeta) + d_2 \cosh(k_1\zeta) + d_3 \sin(|k_2|\zeta) + d_4 \cos(|k_2|\zeta)$$

3) If $k_1^2 < 0$ and $k_2^2 < 0$, then

$$X_u = c_1 \sin(|k_1|\zeta) + c_2 \cos(|k_1|\zeta) + c_3 \sin(|k_2|\zeta) + c_4 \cos(|k_2|\zeta)$$

$$X_v = d_1 \sin(|k_1|\zeta) + d_2 \cos(|k_1|\zeta) + d_3 \sin(|k_2|\zeta) + d_4 \cos(|k_2|\zeta)$$

4) If $k_1^2 = k_2^2 < 0$, then

$$X_u = c_1 \sin(|k_1|\zeta) + c_2 \cos(|k_1|\zeta) + c_3\zeta \sin(|k_1|\zeta) + c_4\zeta \cos(|k_1|\zeta)$$

$$X_v = d_1 \sin(|k_1|\zeta) + d_2 \cos(|k_1|\zeta) + d_3\zeta \sin(|k_1|\zeta) + d_4\zeta \cos(|k_2|\zeta)$$

The sinh and cosh components correspond to near-field (decay) waves and the sine and cosine components correspond to far-field (propagation) waves as discussed by Doyle.[13] This mathematical representation of mode shapes matches the properties of wave propagation of in-plane plate vibration. For example, we consider a plate with a clamped edge at $\zeta = 0$ and a free edge at $\zeta = 1$. The expressions of mode shape functions X_u and X_v are assumed same as the second case for $k_1^2 > 0$ and $k_2^2 < 0$. When these functions are substituted into corresponding boundary conditions as shown in Eqs. (10–12), this yields

$$\begin{bmatrix} 0 & 1 & 0 & 1 \\ e_1 & 0 & -e_2 & 0 \\ p_1\cosh(k_1) & p_1\sinh(k_1) & p_2\cos(k_2) & -p_2\sin(k_2) \\ q_1\sinh(k_1) & q_1\cosh(k_1) & q_2\sin(k_2) & q_2\cos(k_2) \end{bmatrix} \begin{bmatrix} c_1 \\ c_2 \\ c_3 \\ c_4 \end{bmatrix} = 0 \tag{19}$$

where

$$e_1 = -\frac{k_1^2 + a_3}{a_2 k_1}, \qquad e_2 = -\frac{-k_2^2 + a_3}{a_2 k_2}$$

$$p_1 = a_1 k_1 + a_{22} e_1, \qquad p_2 = a_1 k_2 - a_{22} e_2$$

$$q_1 = b_{11} e_1 k_1 + b_{22}, \qquad q_2 = b_{11} e_2 k_2 + b_{22}$$

When nontrivial solutions of Eq. (19) are assumed the resulting four by four determinant is a function in terms of unknown parameter of Ω only. First, we numerically determine an Ω_x resulting in a zero determinant to obtain the modal frequency in the ζ direction. Then, the wave coefficients c_1, c_2, c_3, and c_4 can be solved for this particular frequency Ω_x. Finally, we can construct the mode shape functions X_u and X_v. The next step is to assume that the X_u and X_v pair is prescribed a priori. Similarly, we obtain

$$\delta u = X_u \delta Y_u \tag{20}$$

$$\delta v = X_v \delta Y_v \tag{21}$$

substituting Eqs. (3), (4), (20), and (21) into Eq. (2) and performing integration along the ζ direction. This is the same procedure as we did in the η directions. We show the final two ODEs and associated boundary conditions:

$$f_1 \frac{d^2 Y_u}{d\eta^2} + f_2 \frac{dY_v}{d\zeta} + f_3 Y_u = 0 \tag{22}$$

$$g_1 \frac{d^2 Y_v}{d\eta^2} + g_2 \frac{dY_u}{d\zeta} + g_3 Y_v = 0 \tag{23}$$

The boundary conditions at $\eta = 0, 1$ are needed. For a clamped edge,

$$Y_u = Y_v = 0 \tag{24}$$

For a free edge,

$$g_1 \frac{dY_v}{d\eta} + g_{22} Y_u = 0 \tag{25}$$

$$f_{11} \frac{dY_u}{d\eta} + f_{22} Y_v = 0 \tag{26}$$

where

$$f_1 = \int_0^1 \alpha^2 \frac{1}{2}(1-\nu) X_u^2 \, d\zeta, \qquad f_{11} = \int_0^1 \alpha^2 X_u^2 \, d\zeta$$

$$f_2 = \int_0^1 \frac{1}{2}\alpha(1+\nu)\frac{dX_v}{d\zeta} X_u \, d\zeta - \nu\alpha(X_v X_u)|_{\zeta=0}^1$$

$$f_{22} = \int_0^1 \alpha \frac{dX_v}{d\zeta} X_u \, d\zeta$$

$$f_3 = \int_0^1 \left(\frac{d^2 X_u}{d\zeta^2} X_u + \Omega^2 X_u^2\right) d\zeta - \left(\frac{dX_u}{d\zeta} X_u\right)\Big|_{\zeta=0}^1$$

$$g_1 = \int_0^1 \alpha^2 X_v^2 \, d\zeta$$

$$g_2 = \int_0^1 \frac{1}{2}(1+\nu)\alpha \frac{dX_u}{d\zeta} X_v \, d\zeta - \frac{1}{2}(1-\nu)\alpha(X_u X_v)|_{\zeta=0}^1$$

$$g_{22} = \int_0^1 \alpha \frac{dX_u}{d\zeta} X_v \, d\zeta$$

$$g_3 = \int_0^1 \left[\frac{1}{2}(1-\nu)\frac{d^2 X_v}{d\zeta^2} X_v + \Omega^2 X_v^2\right] d\zeta - \frac{1}{2}(1-\nu)\left(\frac{dX_v}{d\zeta} X_v\right)\Big|_{\zeta=0}^1$$

We follow the same procedure to determine the modal frequency Ω_y and the mode shapes Y_u and Y_v. However, we cannot find the convergent solutions by applying the procedure only once for both directions ζ and η because we wish to have a convergent solution such that $\|\Omega_x^i - \Omega_y^i\| \le \epsilon$. Therefore, an iteration scheme is applied to achieve a convergent solution for both frequency and mode shapes.

Procedure

We summarize our iteration scheme in the following steps:

1) In the η direction, prescribe the mode shape pair Y_u^0 and Y_v^0 a priori, $k = 0$.

2a) Increment k, $Y_u^k = Y_u^{k-1}$, and $Y_v^k = Y_v^{k-1}$.

2b) Obtain the ODEs in terms of X_u^k and X_v^k as shown in Eqs. (8) and (9). Numerically solve for Ω_x^k such that it results in a zero determinant. The wave coefficients in X_u^k and X_v^k are determined under Ω_x^k.

2c) Using mode shape function X_u^k and X_v^k as calculated in step 2b, obtain the ODEs in terms of Y_u^k and Y_v^k as shown in Eqs. (22) and (23). Numerically solve for Ω_y^k such that it results in a zero determinant. The wave coefficients in Y_u^k and Y_v^k can be determined.

3) Check convergence between Ω_x^k and Ω_y^k. If $\|\Omega_x^i - \Omega_y^i\| \le \epsilon$, we stop the iteration. In our calculation, we set $\epsilon = 10^{-5}$. Otherwise, go to step 2a, $k = k + 1$.

Examples

Farag and Pan[9] considered three rectangular plates as shown in Fig. 2: CCCC, CCCF, and CFCF cases. Plate dimensions are 1.0 m in length, 1.2 m in width, and 2.5 mm in thickness. Young's modulus is $E = 70 \times 10^9$ N/m^2 and density is 2700 kg/m^3. Poisson's ratio is $\nu = 0.33$. To validate this method, we will calculate natural frequencies and mode shapes for the in-plane plate vibration problems investigated by them.

To start our approach, we need to discuss how to choose the initial assumed mode shape pair in either the ζ or η direction. Generally speaking, those mode shapes must satisfy two conditions. First, they should be admissible functions, which satisfy the geometric boundary conditions. Second, the resulting coupling coefficients in Eq. (8) or in Eq. (22), that is, a_2 or f_2, cannot be zero. This ensures that we solve the coupled mode shapes as discussed in the preceding

Table 1 Admissible rod mode shape functions

Boundary condition	Mode shape function
CCCC	$W_m = \sin(m\pi x/l)$
CCCF	$W_m = \sin[(2m-1)\pi x/2l]$
CFCF	$W_m = \cos(m\pi x/l)$

Table 2 Natural frequencies of in-plane vibration of a rectangular plate with CCCC boundary conditions

Mode no.	Mode shape for u $m \times n$	Mode shape for v $m \times n$	NASTRAN frequency, Hz	Present		Farag and Pan[9]	
				Frequency, Hz	Error, %	Frequency, Hz	Error, %
1	2 × 2	1 × 1	2658	2667	0.3	2671	0.5
2	1 × 1	2 × 2	2898	2909	0.4	2914	0.6
3	1 × 2	2 × 1	3260	3280	0.6	3349	2.7
4	1 × 2	2 × 1	4024	4089	1.6	4198	4.3
5	1 × 3	2 × 2	4268	4327	1.4	4404	3.2
6	2 × 3	1 × 2	4404	4437	0.7	4607	4.6

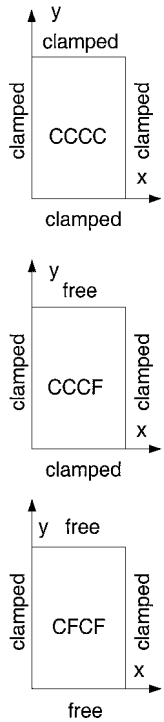

Fig. 2 Three configurations of rectangular plate under in-plane vibration.

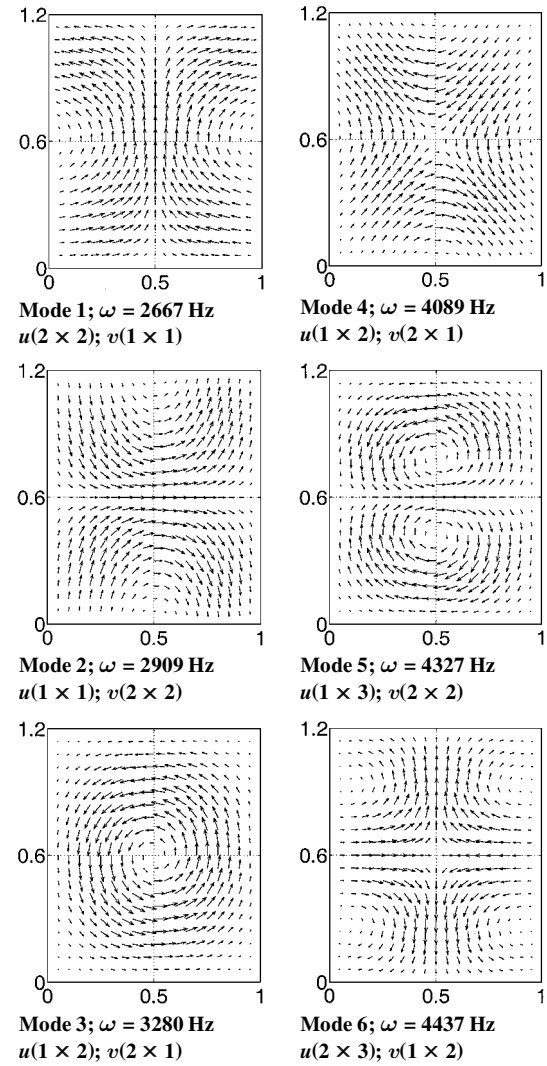

Fig. 3 Mode shapes of in-plane vibration of a rectangular plate with CCCC boundary conditions.

section. The one-dimensional rod vibration mode shapes are used to initialize the iteration calculation and are tabulated for different boundary conditions in Table 1. These rod mode shape functions are admissible functions in the x and y directions. Because of the orthogonality of trigonometric functions as shown in Table 1, the summation of modal number for the assumed pair of Y_u^m and Y_v^n has to be an odd number to satisfy the second criterion for the initial mode pair. The condition $\text{Mod}(m+n)=1$ must hold to achieve nonzero value of a_2 or f_2. Our numerical calculation results validate this remark.

Results

We tabulated the first six natural frequencies of in-plane rectangular plate vibration. All three boundary condition cases were considered. Table 2 shows the natural frequencies of a clamped rectangular plate (CCCC) case. Our results are compared to the solutions of NASTRAN and to those of Farag and Pan.[9] Compared to NASTRAN results, the maximum error is 1.6% in our analysis and 4.6% for Farag and Pan's. Thus, improved accuracy has been achieved in our analysis because the plate mode shapes are more accurate.

Table 3 shows the frequency results of the CCCF case. The error increases for both analyses compared to NASTRAN because a free edge is introduced. Again, the maximum error is 3.9% in our analysis and 8.4% for theirs. However, the maximum error in our analysis are still lower than those of Farag and Pan.[9] Table 4 shows the frequency results of the CFCF case. Our results are improved over Farag and Pan's. The maximum error in Farag and Pan's results reaches 12% compared to 4.5% in our analysis. We demonstrate mode shape functions of the first six modes shapes in Figs. 3–5 for all three cases. These are plotted in vector form. The origin of the arrow denotes the location, and the length of the arrow denotes the magnitude of the resultant displacements. This gives us a visualization of the mode shapes for in-plane plate motion. As shown in Fig. 3 for the CCCC case, we can observe some node lines in which displacement is dominant only in one direction. The displacements are symmetric with respect to those lines for the first, second, fifth, and sixth modes. However, for the third and fourth modes, the shear (rotation) mode shape is easily identified. The third mode corresponds to the rotation with respect to the center of a plate. For the fourth mode, the displacements behave similarly to the case in which the extension and compression occurs along two diagonals of a plate. For the CCCF case, as shown in Fig. 4, the mode shape

Table 3 Natural frequencies of in-plane vibration of a rectangular plate with CCCF boundary conditions

Mode no.	Mode shape for u $m \times n$	Mode shape for v $m \times n$	NASTRAN frequency, Hz	Present		Farag and Pan[9]	
				Frequency, Hz	Error, %	Frequency, Hz	Error, %
1	2×2	1×1	1803	1811	0.4	1892	4.9
2	1×1	2×2	2656	2674	0.7	2727	2.7
3	1×2	2×1	2794	2845	1.8	3026	8.4
4	1×2	2×1	3392	3524	3.9	3596	6.0
5	2×3	1×2	3479	3504	0.7	3624	4.2
6	1×3	2×2	3704	3757	1.4	3868	4.4

Table 4 Natural frequencies of in-plane vibration of a rectangular plate with CFCF boundary conditions; modal number 0 denotes the rigid mode

Mode no.	Mode shape for u $m \times n$	Mode shape for v $m \times n$	NASTRAN frequency, Hz	Present		Farag and Pan[9]	
				Frequency, Hz	Error, %	Frequency, Hz	Error, %
1	2×3	1×0	1449	1455	0.4	1531	7.0
2	2×2	1×1	2511	2520	0.4	2682	6.0
3	1×0	2×1	2567	2639	2.8	2697	5.0
4	1×1	2×0	2637	2662	0.95	2994	12.0
5	1×1	2×0	3037	3187	4.5	3122	3.0
6	1×2	2×1	3061	3146	2.8	3390	10.0

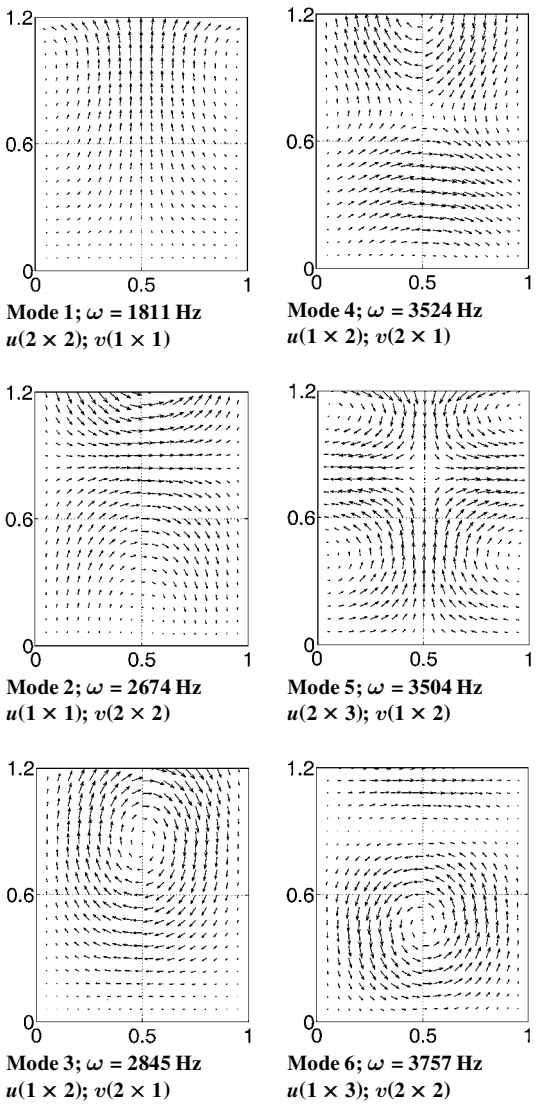

Mode 1; ω = 1811 Hz **$u(2 \times 2)$; $v(1 \times 1)$**

Mode 4; ω = 3524 Hz **$u(1 \times 2)$; $v(2 \times 1)$**

Mode 2; ω = 2674 Hz **$u(1 \times 1)$; $v(2 \times 2)$**

Mode 5; ω = 3504 Hz **$u(2 \times 3)$; $v(1 \times 2)$**

Mode 3; ω = 2845 Hz **$u(1 \times 2)$; $v(2 \times 1)$**

Mode 6; ω = 3757 Hz **$u(1 \times 3)$; $v(2 \times 2)$**

Fig. 4 Mode shapes of in-plane vibration of a rectangular plate with CCCF boundary conditions.

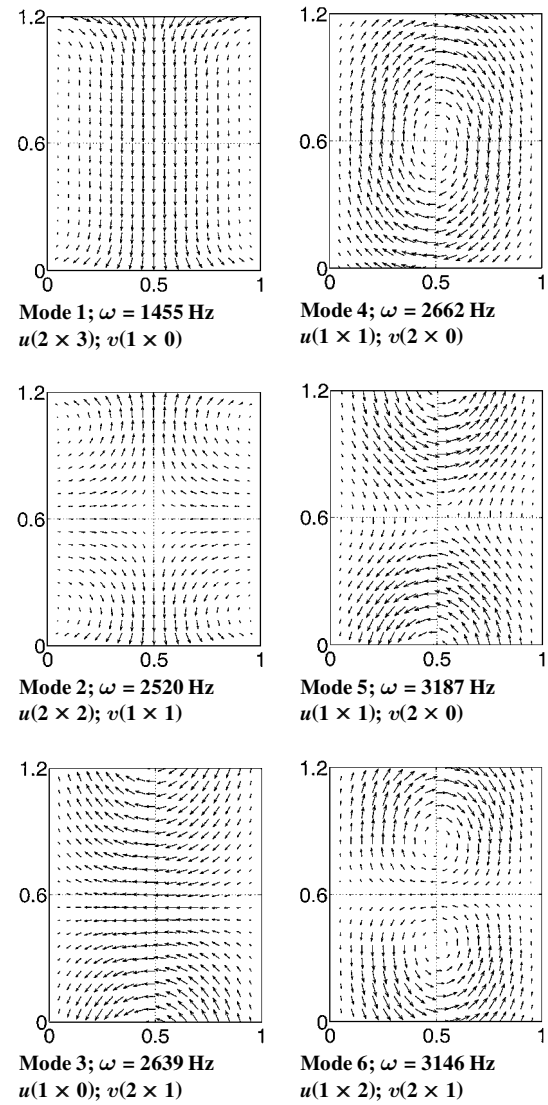

Mode 1; ω = 1455 Hz **$u(2 \times 3)$; $v(1 \times 0)$**

Mode 4; ω = 2662 Hz **$u(1 \times 1)$; $v(2 \times 0)$**

Mode 2; ω = 2520 Hz **$u(2 \times 2)$; $v(1 \times 1)$**

Mode 5; ω = 3187 Hz **$u(1 \times 1)$; $v(2 \times 0)$**

Mode 3; ω = 2639 Hz **$u(1 \times 0)$; $v(2 \times 1)$**

Mode 6; ω = 3146 Hz **$u(1 \times 2)$; $v(2 \times 1)$**

Fig. 5 Mode shapes of in-plane vibration of a rectangular plate with CFCF boundary conditions.

displacements showed the different results compared to the CCCC case. Because of an introduction of a free edge, the displacements are smaller close to the clamped edges and become larger when reaching the free edge. The mode shapes lose some symmetries. The symmetric shape exists only in the vertical direction, as shown in the first and fifth modes of the CCCF case. For the CFCF case, as shown in Fig. 5, similar results are obtained compared to the CCCC case. We can identify the node lines and the properties of symmetry easily. The displacements become yet larger when reaching two free edges.

Conclusions

Based on the Kantorovich–Krylov method, we computed the natural frequencies and natural modes of rectangular plates. The analytical results were validated using both NASTRAN and results from the literature.[9] Improved accuracy for the natural frequency calculations for three cases was achieved when compared to available results from literature relative to the NASTRAN analysis. Mode shapes were expressed as a linear combination of wave propagation where the wave coefficients were computed using a numerical iteration scheme. The mode shapes were given in the analytical forms in which the wave coefficients were determined through a numerical iteration scheme:

1) As shown in Table 2 for the CCCC case, the maximum error of our analysis was 1.6 and 4.6% for Farag and Pan's[9] analysis. Both analyses predict natural frequency well.

2) As shown in Table 3 for the CCCF case, the maximum error of our analysis was 3.9 and 8.4% for Farag and Pan's[9] analysis. The errors in the CCCF case increase for both analyses. The introduction of a free edge increases the displacement coupling because a force boundary condition exists.

3) As shown in Table 4 for the CFCF case, the maximum error continues to increase, 4.5% in our analysis and 12% in Farag and Pan's.[9] As more free edges are added, the coupling effects between mode shapes increase.

Overall, more accurate frequency calculations were achieved in our analysis relative to the NASTRAN analysis. The plots of mode shapes provide us with a visualization of displacement field for in-plane plate vibration. Therefore, we have successfully solved the in-plane vibration problem of rectangular plates. The present analysis lays the groundwork for future investigation of in-plane plate vibration coupled with other motions.

Acknowledgments

This research was supported by the U.S. Army Research Office under the FY96 Multidisciplinary University Research Initiative in Active Control of Rotorcraft Vibration and Acoustics (Gary Anderson and Tom Doligalski, Technical Monitors). Laboratory equipment support was provided under the FY96 Defense University Research Instrumentation Program, Contract DAAH-0496-10301 (Gary Anderson, Technical Monitor). We also thank A. W. Leissa (Ohio State University) for his helpful discussions on this topic.

References

[1]Leissa, A., "Vibration of Plates," NASA SP-160, 1969.

[2]Blevin, R. D., *Formulas for Natural Frequency and Mode Shape*, Van Nostrand Reinhold, 1979, pp. 233–290.

[3]Leung, A. Y. T., *Dynamic Stiffness and Substructures*, Springer-Verlag, London, 1993, pp. 34–39.

[4]Bercin, A. N., and Langley, R. S., "Application of the Dynamic Stiffness Technique to the In-Plane Vibrations of Plate Structures," *Computers and Structures*, Vol. 59, No. 5, 1996, pp. 869–875.

[5]Wang, G., Veeramani, S., and Wereley, N. M., "Analysis of Sandwich Plates with Isotropic Face Plates and a Viscoelastic Core," *Journal of Vibration and Acoustics*, Vol. 122, No. 3, 2000, pp. 305–312.

[6]Wang, G., "Analyses of Sandwich Beam and Plate with Viscoelastic Cores," Ph.D. Dissertation, Dept. of Aerospace Engineering, Univ. of Maryland, College Park, MD, Dec. 2001.

[7]Graff, K. F., *Wave Motion in Elastic Solids*, Clarendon, Oxford, 1975, pp. 435–458.

[8]Farag, N. H., and Pan, J., "Free and Forced In-Plane Vibration of Rectangular Plates," *Journal of the Acoustical Society of America*, Vol. 103, No. 1, 1998, pp. 408–413.

[9]Farag, N. H., and Pan, J., "Modal Characteristics of In-Plane Vibration of Rectangular Plates," *Journal of the Acoustical Society of America*, Vol. 105, No. 6, 1999, pp. 3295–3309.

[10]Kantorovich, L. V., and Krylov, V. I., *Approximate Methods of Higher Analysis*, Noordhoff International, Groningen, The Netherlands, 1964, pp. 241–357.

[11]Bhat, R. B., Singh, J., and Mundkur, G., "Plate Characteristic Functions and Natural Frequencies of Vibration of Plates by Iterative Reduction of Partial Differential Equation," *Journal of Vibration and Acoustics*, Vol. 115, No. 2, 1993, pp. 177–181.

[12]Washizu, K., *Variational Methods in Elasticity and Plasticity*, Pergamon, New York, 1968, pp. 152–181.

[13]Doyle, J. F., *Wave Propagation in Structures*, 2nd ed., Springer-Verlag, New York, 1997, Chap. 4.

A. Berman
Associate Editor